FEBS 21635 FEBS Letters 445 (1999) 431–439

Visualization of caveolin-1, a caveolar marker protein, in living cells using green fluorescent protein (GFP) chimeras

The subcellular distribution of caveolin-1 is modulated by cell-cell contact

Daniela Volontè, Ferruccio Galbiati, Michael P. Lisanti*

Department of Molecular Pharmacology and The Albert Einstein Cancer Center, Albert Einstein College of Medicine, 1300 Morris Park Avenue, Bronx, NY 10461, USA

Received 19 January 1999; received in revised form 27 January 1999

Abstract Caveolin-1, a suspected tumor suppressor, is a principal protein component of caveolae in vivo. Recently, we have shown that NIH 3T3 cells harboring anti-sense caveolin-1 exhibit a loss of contact inhibition and anchorage-independent growth. These observations may be related to the ability of caveolin-1 expression to positively regulate contact inhibition. In order to understand the postulated role of caveolin-1 in contact inhibition, it will be necessary to follow the distribution of caveolins in living cells in response to a variety of stimuli, such as cell density. Here, we visualize the distribution of caveolin-1 in living normal NIH 3T3 cells by creating GFP-fusion proteins. In many respects, the behavior of these GFP-caveolin-1 fusion proteins is indistinguishable from endogenous caveolin-1. These GFP-caveolin-1 fusion proteins co-fractionated with endogenous caveolin-1 using an established protocol that separates caveolae-derived membranes from the bulk of cellular membranes and cytosolic proteins, and co-localized with endogenous caveolin-2 in vivo as seen by immunofluorescence microscopy. We show here that as NIH 3T3 cells become confluent, the distribution of GFP-caveolin-1 and endogenous caveolin-1 shifts to areas of cell-cell contact, coincident with contact inhibition. However, unlike endogenous caveolin-1, the levels of GFP-caveolin-1 expression are unaffected by changes in cell density, serum starvation, or growth factor stimulation. These results are consistent with the idea that the levels of endogenous caveolin-1 are modulated by either transcriptional or translational control, and that this modulation is separable from density-dependent regulation of the distribution of caveolin-1. These studies provide a new living-model system for elucidating the dynamic mechanisms underlying the density-dependent regulation of the distribution of caveolin-1 and how this relates to contact inhibition.

Key words: Caveolin-1; Green fluorescent protein

1. Introduction

Caveolae, the 'little caves' first described in electron micrographs of endothelial cells, have emerged in recent years as the site of the important dynamic or regulatory events at the plasma membrane [1–3]. Both transcytosis and potocytosis occur within these cell surface organelles, as does the uptake of oxidized low density lipoprotein particles via endothelial scavenger receptors, the uptake of cholera toxin and DNA tumor viruses, the processing of Alzheimer disease-related protein APP, and of the scrapie prion protein PrP [4–9].

Caveolae have also been implicated in signal transduction, particularly by receptor tyrosine kinases and G proteins [2]. Caveolae are enriched in specific lipids (glyco-sphingolipids, sphingomyelin and cholesterol) and lipid-modified signaling molecules relative to the rest of the cell surface. Due to this distinctive protein and lipid profile, plasma membrane caveolae are detergent-insoluble and can be purified away from other cellular membranes by sucrose density gradient centrifugation. Caveolae can also be prepared using detergent-free methods [10], such as affinity purification using a recombinant form of caveolin-1 [11]. GPI domains are separated from caveolae using this detergent-free procedure, as evidenced by exclusion of GPI-anchored carbonic anhydrase IV [11]. These caveolae-enriched membrane domains contain lipid-modified signaling molecules (G-proteins, Src-tyrosine kinases, H-Ras and eNOS) [2,11].

Caveolins, a family of highly conserved integral membrane proteins, interact specifically with these signaling molecules and many of their binding partners, apparently providing a scaffold that places members of a signal transduction pathway in close proximity with one another. The mammalian caveolin gene family consists of caveolins-1, -2, and -3 [2,12–14]. Caveolins 1 and 2 are co-expressed and form a hetero-oligomeric complex [15] in many cell types, with particularly high levels in adipocytes, whereas expression of caveolin-3 is muscle-specific and found in both cardiac and skeletal muscle, as well as smooth muscle cells [16].

Caveolae-like vesicles can be generated by expressing caveolin-1 or -3 in insect cells using a baculovirus based expression system, or in mammalian cell lines [17–20], providing an in vivo assay for caveolin-dependent vesicle formation. In addition, caveolin-induced vesicle formation appears to be isoform-specific. Expression of caveolin-2 alone under the same conditions failed to drive the formation of vesicles [19,20], either in insect cells or in mammalian cell systems.

Accumulating evidence suggests that caveolins possess all the qualities of scaffolding proteins. Caveolins form multivalent homo- and hetero-oligomers and each caveolin-interacting protein binds to the same cytosolic membrane-proximal region of caveolin [21,22]. Domain-mapping studies have revealed that the interaction of caveolin-1 with signaling molecules is mediated via a membrane proximal region of caveolin, termed the caveolin-scaffolding domain (residues 82–101). Through this domain, caveolin-1 interacts with G-protein α subunits, H-Ras, Src family tyrosine kinases, PKC isoforms, EGF-R, Neu, and eNOS (reviewed in [2,23,24]). In many cases, it has been shown that mutational activation of these signaling molecules (G-proteins, H-Ras, or Src family kinases)

*Corresponding author. Fax: (1) (718) 430 8830.
E-mail: lisanti@aecom.yu.edu

PII: S0014-5793(99)00164-7

prevents regulated interaction with the caveolin-scaffolding domain [11,22,25]. These activating mutations include H-Ras (G12V) and $G\alpha_s$ (Q227L) that are found in human cancers.

The caveolin-scaffolding domain recognizes a well defined caveolin-binding motif that includes several crucial aromatic amino acid residues [3,26,27]. This motif was identified by using the caveolin-scaffolding domain to select random peptide ligands from phage display libraries [3,26,27]. The relevance of the motif we identified was stringently evaluated using a well-characterized caveolin-binding protein, namely a G-protein α subunit ($G\alpha_{i2}$). Since the identification of the caveolin-scaffolding domain [22] and caveolin-binding sequence motifs [3,26,27], these observations have been extended to other caveolin-interacting proteins. Functional caveolin-binding motifs have been deduced in both tyrosine and serine/threonine kinases, as well as eNOS [2,27,28]. In all cases examined, the caveolin binding motif is located within the enzymatically active catalytic domain of a given signaling molecule. For example, in the case of tyrosine and serine/threonine kinases, a kinase domain consists of 11 conserved subdomains (I–XI), and the caveolin binding motif occurs within subdomain IX [3,26,27]. Caveolin-binding via the scaffolding domain is sufficient to inhibit the enzymatic activity of these kinases in vitro. Indeed, in many cases, a synthetic peptide corresponding to this caveolin domain is the most potent peptide inhibitor known for these enzymes. Agents that mimic the interaction with caveolins are potentially useful as general kinase inhibitors, and possibly as anti-tumor drugs.

Recognition of signaling molecules by the caveolins also appears to be isoform-specific. Scaffolding domains of caveolins-1 and -3 recognize a common motif, which does not interact with caveolin-2 [3,26,27]. Conversely, certain isoforms of PKC lack a defined caveolin-binding motif and thus are not inhibited by the caveolin-scaffolding domain [28]. Alanine scanning mutagenesis of the caveolin-scaffolding domain has revealed that the sequence FTVT/S is essential for proper recognition of caveolin binding motifs; this sequence is conserved in caveolins-1 and -3 and is divergent in caveolin-2 (FEIS) [3,26,27]. Recently, we have identified a family with an autosomal dominant form of limb girdle muscular dystrophy [29]. In this family, the FTVT/S region is deleted in caveolin-3, providing genetic evidence that this region of the caveolin-scaffolding domain is critical in vivo.

The in vivo relevance of the caveolin-binding motif within eNOS has recently been tested functionally [30]. The caveolin-binding motif within eNOS was removed by site-directed mutagenesis by substituting alanine in place of important aromatic residues that are required for recognition by caveolins. Removal of the eNOS caveolin-binding motif did not affect the basal enzymatic activity of eNOS, but it did block the ability of caveolin-1 to suppress eNOS activity in co-transfection experiments [30]. This is the first demonstration showing that the caveolin-scaffolding domain and caveolin-binding sequence motifs are functional in vivo. These NOS-caveolin interactions have been shown to be relevant in both endothelial cells and cardiac myocytes, that are known to express caveolins-1 and -3, respectively.

Modification and/or inactivation of caveolin-1 expression appears to be a common feature of the transformed phenotype. Caveolin-1 mRNA and protein expression are reduced or absent in NIH 3T3 cells transformed by a variety of activated oncogenes (v-Abl, Bcr-Abl, H-Ras (G12V)), and caveolae are also missing from these transformed cells [31]; caveolin-2 protein is not down-regulated in response to oncogenic transformation [15]. In addition, caveolin-1 expression levels correlated inversely with the ability of these cells to grow in soft agar. Thus, cells expressing the smallest amount of caveolin-1 and lacking detectable caveolae formed the largest colonies in soft agar. These observations suggest that functional alterations in caveolae may play a critical role in oncogenic transformation, perhaps by disrupting contact inhibition in transformed cells [31].

Down-regulation of caveolin-1 is a direct consequence of the oncogenic stimulus as it can be reversed by employing a temperature sensitive form of v-Abl or by treating Ras-transformed 3T3 cells with an inhibitor of the p42/44 MAP kinase pathway (PD 98059). Re-introduction of caveolin-1 under the control of an inducible expression system is sufficient to block the anchorage-independent growth of these transformed cells in soft agar and restore the formation of morphologically detectable caveolae [20]. Consistent with its antagonism of Ras-mediated cell transformation, caveolin-1 expression dramatically inhibited both Ras/MAPK-mediated and basal transcriptional activation of a mitogen-sensitive promoter [20]. Taken together, these results clearly indicate that down-regulation of caveolin-1 expression and caveolae organelles may be critical to maintaining the transformed phenotype in certain cell populations [20]. In support of these findings, the human gene encoding caveolin-1 has recently been localized to suspected tumor suppressor locus (D7S522; chromosome 7q31.1) that is frequently deleted in a variety of human cancers [32,33].

The above observations may be related to the ability of caveolin-1 to positively regulate contact inhibition and growth arrest in normal cells [34]. Recently, we have shown that both the distribution and the expression of endogenous caveolin-1 are dramatically altered at confluence in normal NIH 3T3 cells [34]. These results are consistent with the idea that caveolin-1 expression may be important to mediate normal contact inhibition and to negatively regulate the activation state of the Ras-p42/44 MAP kinase cascade [34].

Here, we visualize the distribution of exogenous caveolin-1 in living NIH 3T3 cells by creating GFP-caveolin-1 fusion proteins. These constructs were carefully characterized by transient expression in the non-transformed murine fibroblastic NIH 3T3 cell line, which normally contains caveolae, expresses endogenous caveolins-1 and -2, and is contact inhibited for growth in vitro. We show that as these normal NIH 3T3 cells become confluent, the distribution of GFP-caveolin-1 and endogenous caveolin-1 shifts to areas of cell-cell contact, coincident with contact inhibition. This is the first demonstration that caveolins can be visualized in living cells using GFP chimeras and that these GFP-caveolin-1 fusions mimic the behaviour of endogenous caveolin-1 in vivo.

2. Materials and methods

2.1. Materials

Antibodies and their sources were as follows: anti-caveolin-1 IgG (mAb 2297; gift of John R. Glenney, Jr., Transduction Laboratories [35]); anti-caveolin-2 IgG (mAb 65; gift of John R. Glenney, Jr., Transduction Laboratories [15]); anti-GFP IgG (pAb, Clontech, Inc.).

2.2. Cell culture

NIH 3T3 cells were grown in DME supplemented with 2 mM

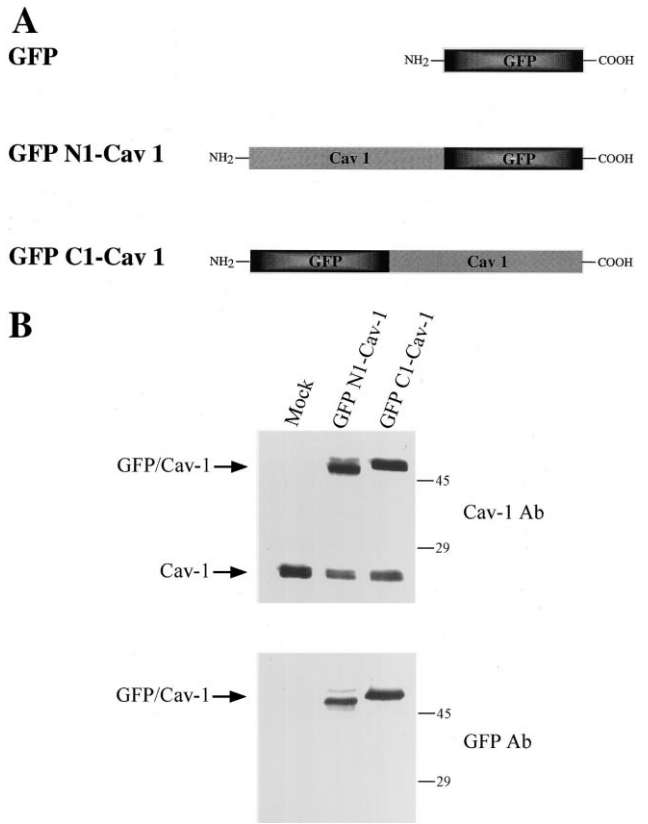

Fig. 1. Construction and expression of GFP-caveolin-1 fusion proteins. A: Schematic diagram showing the construction of GFP-caveolin-1 fusion proteins. The entire coding region of canine caveolin-1 was placed in-frame either at the N-terminal or the C-terminal end of GFP, to create GFP N1-Cav-1 and GFP C1-Cav-1, respectively. B: GFP-caveolin-1 fusion proteins were transiently expressed in NIH 3T3 cells using a standard calcium phosphate precipitation protocol. Cell lysates were prepared and subjected to immunoblot analysis with antibodies directed against either GFP (lower panel) or caveolin-1 (mAb 2297; upper panel). Note that the GFP antibody recognizes only the GFP-caveolin-1 fusions, while the caveolin-1 antibody recognizes both the GFP-caveolin-1 fusions and endogenous caveolin-1.

glutamine, 100 U/ml penicillin, 100 μg/ml streptomycin and 10% donor calf serum [20,31,34].

2.3. Construction of GFP-Cav 1 fusion proteins

The full-length untagged cDNA encoding murine caveolin-1 was fused in-frame either N-terminally or C-terminally to GFP using the pEGFP-N1 vector or the pEGFP-C1 vector (Clontech, Inc.), respectively. NIH 3T3 cells were transfected with either pEGFP-N1 Cav-1 or pEGFP-C1 Cav-1 using a modified calcium phosphate precipitation protocol.

2.4. Immunostaining of NIH 3T3 cells

NIH 3T3 cells were washed three times with PBS and fixed for 30 min at room temperature with 2% paraformaldehyde in PBS. Fixed cells were rinsed with PBS and permeabilized with 0.1% Triton X-100, 0.2% BSA for 10 min. Cells were then treated with 25 mM NH_4Cl in PBS for 10 min at room temperature to quench free aldehyde groups. Cells were rinsed with PBS and incubated with primary antibodies for 1 h at room temperature: either anti-caveolin-1 IgG (pAb; directed against caveolin-1 residues 2–21; Santa Cruz Biotech. Inc.), and/or anti-caveolin-2 IgG (mAb; clone 65, Transduction Laboratories [15]) diluted into PBS with 0.1% Triton X-100, 0.2% BSA. After three washes with PBS (10 min each), cells were incubated with secondary antibodies for 1 h at room temperature: lissamine, rhodamine B, sulfonyl chloride-conjugated goat anti-rabbit antibody (5 μg/ml) and fluorescein isothiocyanate-conjugated goat anti-mouse antibody (5 μg/ml). Cells were washed three times with PBS (10 min each). Slides were mounted with slow-Fade anti-fade reagent and examined by confocal microscopy.

2.5. Serum starvation and growth factor stimulation

NIH 3T3 cells were transfected with either pEGFP-N1 Cav-1 or pEGFP-C1 Cav-1. After 24 h cells were trypsinized and re-plated at a dilution of 1:15 (sparse); after 6 h of culture, complete medium was replaced with medium without serum. Cells were then grown in me-

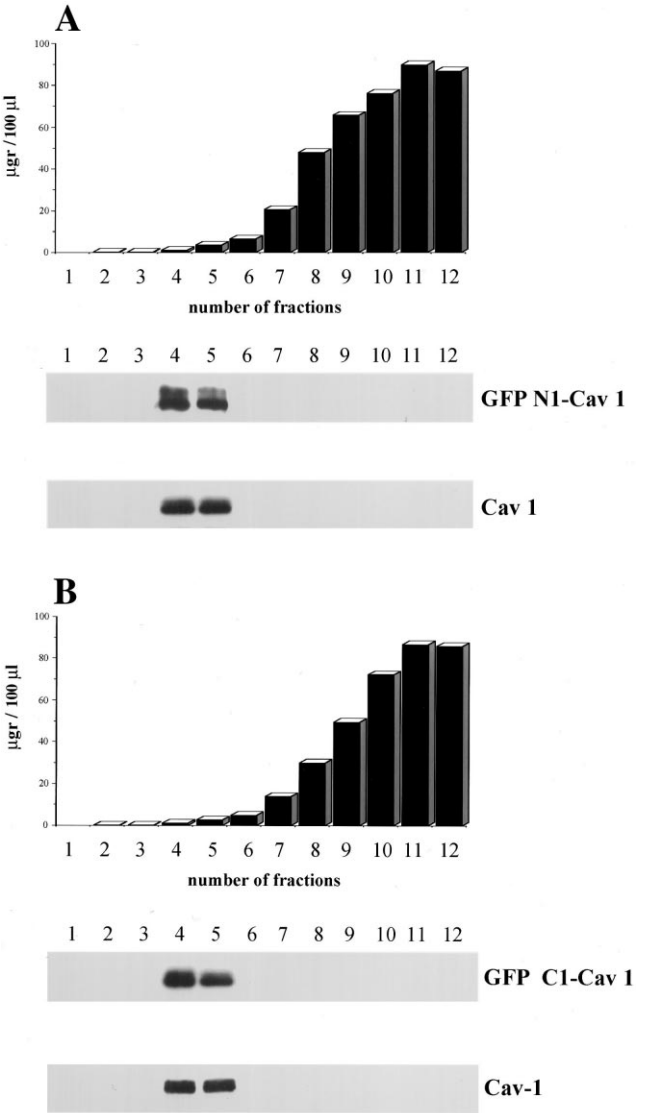

Fig. 2. Co-fractionation of GFP-caveolin-1 fusion proteins with endogenous caveolin-1. NIH 3T3 cells were transiently transfected with the cDNAs encoding GFP-caveolin-1 fusion proteins and subjected to subcellular fractionation. We analyzed the distribution of GFP-caveolin-1 and endogenous caveolin-1 in these transfected cells using an established biochemical procedure that separates caveolae and caveolae-related domains from the bulk of cellular membranes and cytosolic proteins. In this fractionation scheme, immunoblotting with anti-caveolin-1 IgG can be used to track the position of caveolae-derived membranes within these bottom-loaded sucrose gradients. Note that both GFP-caveolin-1 fusion proteins and endogenous caveolin-1 co-fractionate and are confined to the caveolae-enriched fractions (fractions 4 and 5), which exclude $>99.95\%$ of total cellular protein. A: GFP N1-Cav-1; B: GFP C1-Cav-1; upper panels: protein distribution across the gradient; lower panels, Western blot analysis showing the distribution of GFP-caveolin-1 and endogenous caveolin-1.

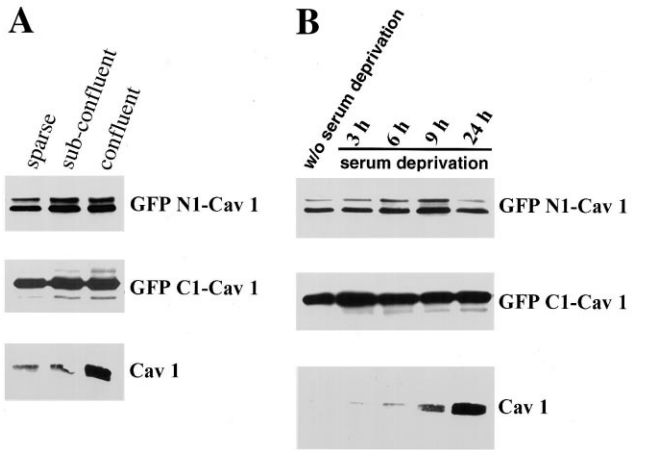

Fig. 3. Differential effects of cell density and serum starvation on the expression of GFP-caveolin-1 fusions and endogenous caveolin-1. A: Effects of cell density: sparse, sub-confluent and confluent. Note that the expression levels of the GFP-caveolin-1 fusion proteins are independent of cell density, while the level of endogenous caveolin-1 increases as the cells reach confluence. B: Effects of serum starvation. Note that the expression levels of the GFP-caveolin-1 fusion proteins are unaffected by serum deprivation, while the levels of endogenous caveolin-1 increase in response to serum deprivation. In panels A and B, each lane contains equal amounts of total protein.

dium without serum for 3, 6, 9 and 24 h, harvested and subjected to immunoblot analysis. In the growth factor stimulation experiments, cells were grown in medium without serum for 24 h in presence or absence of EGF (10 ng/ml) and PDGF (10 ng/ml) in combination.

2.6. In vivo fluorescence microscopy.

NIH 3T3 cells were transfected with either the pEGFP-N1 Cav-1 or pEGFP-C1 Cav-1 vector. After 48 h cells were observed 'in vivo' at an excitation wavelength of 488 nm.

2.7. Immunoblot analysis

Cellular proteins were resolved by SDS-PAGE (12.5% acrylamide) and transferred to nitrocellulose membranes. Blots were incubated for 2 h in TBST (10 mM Tris-HCl, pH 8.0, 150 mM NaCl, 0.2% Tween 20) containing 2% powdered skimmed milk and 1% bovine serum albumin. After three washes with TBST, membranes were incubated for 2 h with the primary antibody (~1000-fold diluted in TBST) and for 1 h with horseradish peroxidase-conjugated goat anti-rabbit/mouse IgG (~5000-fold diluted). Proteins were detected using the ECL detection kit (Amersham).

2.8. Preparation of caveolin-enriched membrane fractions

NIH 3T3 cells were scraped into 2 ml of MES-buffered saline (MBS, 25 mM MES, pH 6.5, 0.15 M NaCl) containing 1% (v/v) Triton X-100 [4,25,35–42]. Homogenization was carried out with 10 strokes of a loose-fitting Dounce homogenizer. The homogenate was adjusted to 40% sucrose by the addition of 2 ml of 80% sucrose prepared in MBS and placed at the bottom of an ultracentrifuge tube. A 5–30% linear sucrose gradient was formed above the homogenate and centrifuged at 39 000 rpm for 16–20 h in a SW41 rotor (Beckman Instruments). A light scattering band confined to the 15–20% sucrose region was observed that contained caveolin-1, but excluded most of other cellular proteins. From the top of each gradient, 1 ml gradient fractions were collected to yield a total of 12 fractions. An equal volume of each gradient fraction was separated by SDS-PAGE and subjected to immunoblot analysis.

3. Results and discussion

3.1. Construction and expression of GFP-caveolin-1 fusion proteins in NIH 3T3 fibroblasts

Fig. 1A shows a schematic diagram summarizing the construction of GFP-caveolin-1 fusion proteins. The cDNA containing the entire coding sequence for canine caveolin-1 was placed in-frame, either at the N-terminal or the C-terminal end of GFP, to create GFP N1-Cav-1 and GFP C1-Cav-1, respectively. As GFP has a molecular mass of ~26–27 kDa, these GFP-caveolin-1 fusions are expected to a have a cumulative molecular mass of ~45–50 kDa.

In order to evaluate the expression of these GFP fusion proteins, these constructs were transiently expressed in NIH 3T3 cells using the calcium phosphate precipitation method. Expression of these GFP-caveolin-1 fusions was monitored by Western blotting using specific antibodies that recognize either GFP or caveolin-1 (mAb 2297).

Fig. 1B shows that both GFP N1-Cav-1 and GFP C1-Cav-1 were well expressed using this approach. Note that both GFP fusion proteins were easily detected with either anti-GFP or anti-caveolin-1 and had an apparent molecular mass of ~45 kDa. Importantly, the GFP-caveolin-1 fusions were not over-expressed using this approach and were expressed at levels that are comparable to endogenous caveolin-1 (Fig. 1B, upper panel).

Note that no bands migrating in the molecular mass range expected for GFP alone (~24–26 kDa) were observed indicating that the GFP-caveolin-1 fusion is relatively stable and is not proteolytically cleaved into GFP and caveolin-1, as has

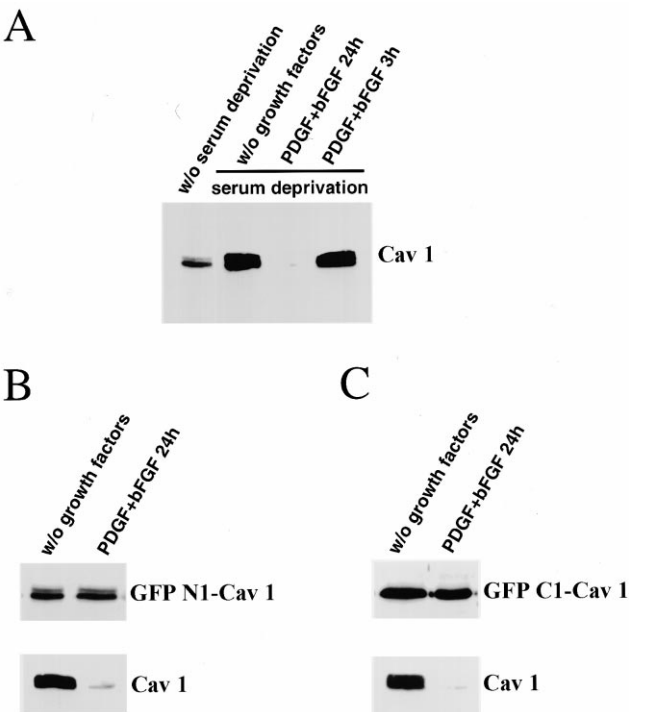

Fig. 4. Differential effects of growth factor stimulation on the expression of GFP-caveolin-1 fusions and endogenous caveolin-1. A: Untransfected NIH 3T3 cells were incubated with or without specific growth factors (PDGF and bFGF) in serum-free medium. Note that caveolin-1 protein levels were dramatically down-regulated after 24 h of growth factor stimulation. B and C: As in panel A, except NIH 3T3 cells were transiently transfected with GFP N1-Cav-1 or GFP C1-Cav-1, respectively. The expression of endogenous caveolin-1 in these transfected cells is shown for comparison. Note that GFP-caveolin-1 fusion proteins are unaffected by growth factor stimulation, while the levels of endogenous caveolin-1 decrease dramatically in response to growth factor stimulation. In panels A–C, each lane contains equal amounts of total protein.

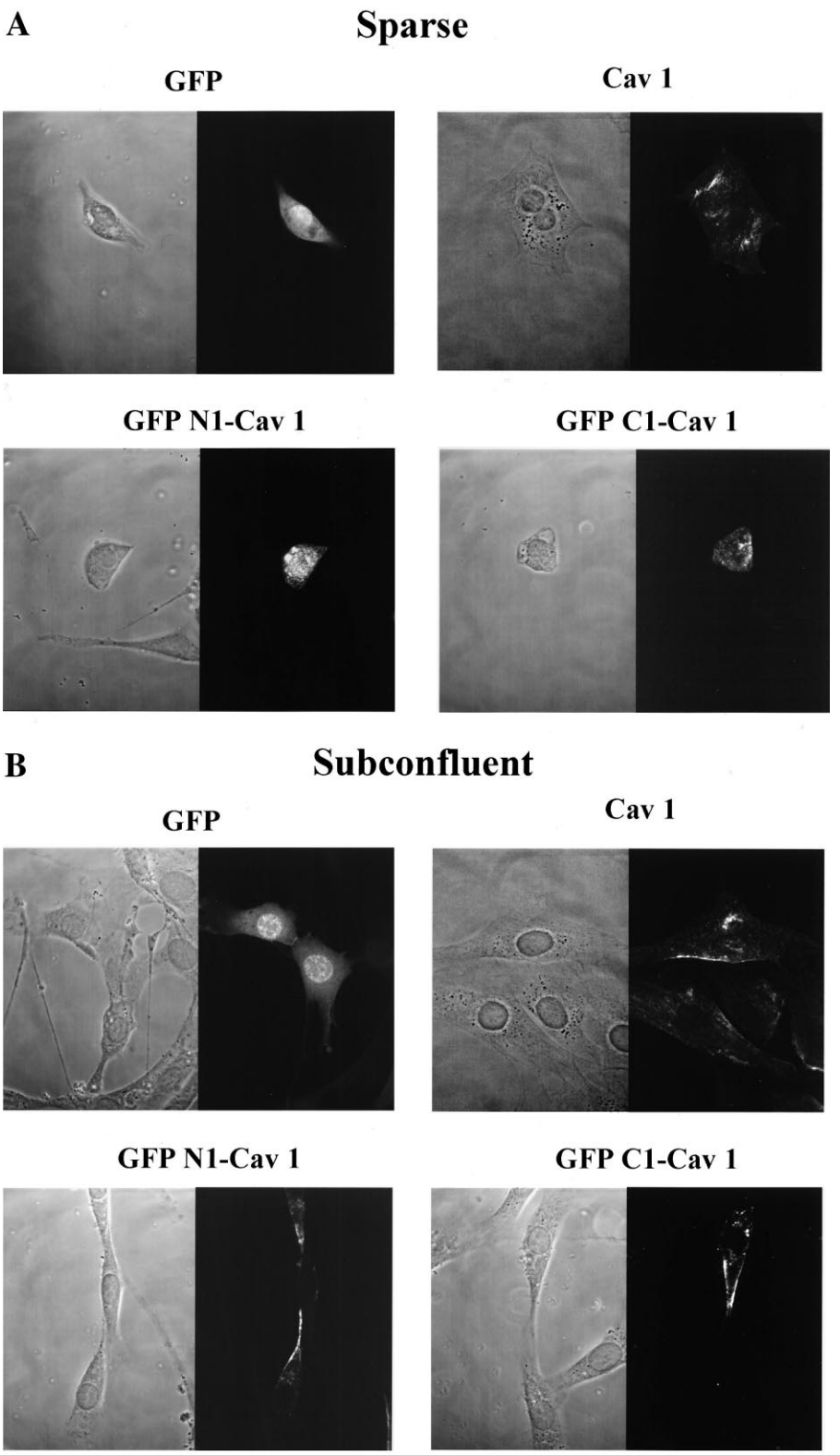

Fig. 5. Localization of GFP, GFP-caveolin-1 fusions, and endogenous caveolin-1 in NIH 3T3 cells: effects of cell density. A: Sparse; B: Subconfluent; C: Confluent. As the cells reach confluence, the distribution of caveolin-1 changes from a uniform punctate distribution over the entire cell surface and becomes localized primarily to areas of cell-cell contact, coincident with contact inhibition. Note that GFP-caveolin-1 fusions mimic the behavior of endogenous caveolin-1; the distribution of GFP alone is shown for comparison. Upper left, GFP alone; upper right, endogenous caveolin-1; lower left, GFP N1-Cav-1; lower right, GFP C1-Cav-1. Phase and the corresponding fluorescence image are shown.

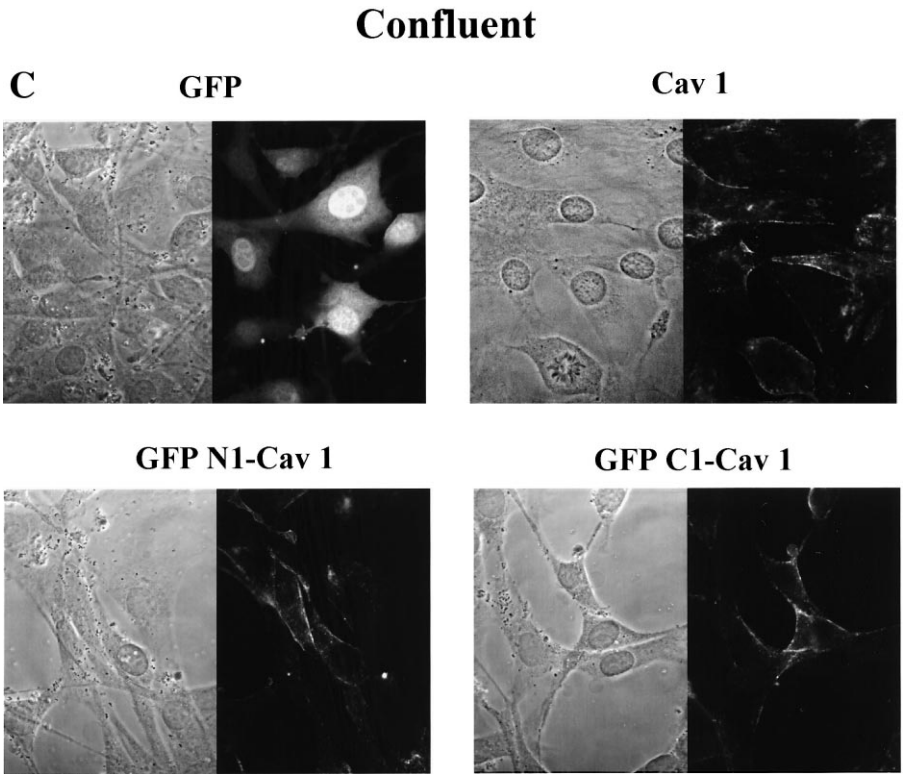

Fig. 5 (*continued*).

been the case with other GFP fusion proteins (Fig. 1B, upper panel). However, GFP N1-Cav-1 and GFP C1-Cav-1 did migrate with slightly different apparent molecular masses; this may be attributed in part to the length of the linker sequence that joins GFP and caveolin-1 which is inherently different depending on their placement N- or C-terminal with respect to GFP. As a consequence, we evaluated the behavior of both GFP-caveolin-1 fusions in parallel and compared them with the behavior of endogenous caveolin-1 using a variety of established approaches, such as cell fractionation and immunofluorescence microscopy.

3.2. Co-fractionation of GFP-caveolin-1 fusion proteins with endogenous caveolin-1

Next, we analyzed the distribution of GFP-caveolin-1 fusions and endogenous caveolin-1 in transiently transfected NIH 3T3 cells using an established biochemical procedure that separates caveolae and caveolae-related domains from the bulk of cellular membranes and cytosolic proteins [4,25,35–43]. In this fractionation scheme, immunoblotting with anti-caveolin-1 IgG can be used to track the position of caveolae-derived membranes within these bottom-loaded sucrose gradients. Using this procedure, caveolin-1 is purified ~2000-fold relative to total cell lysates as ~4–6 μg of caveolin-rich domains (containing ~90–95% of total cellular caveolin-1) are obtained from 10 mg of total cellular proteins [25,39]. We and others have shown that these caveolin-rich fractions exclude >99.95% of total cellular proteins and also markers for non-caveolar plasma membrane, Golgi, lysosomes, mitochondria and endoplasmic reticulum [4,36,38].

Fig. 2 shows that both GFP-caveolin-1 fusion proteins were correctly targeted to caveolae membranes (fractions 4 and 5; lower panels), while excluding greater than 99.95% of total cellular proteins. Note that the distribution of GFP N1-Cav-1 (Fig. 2A) and GFP C1-Cav-1 (Fig. 2B) and distribution of endogenous caveolin-1 is virtually identical in these bottom-loaded sucrose density gradients. These results indicate that the behavior of the GFP-caveolin-1 fusion proteins mimics the behavior of endogenous caveolin-1 to a first approximation. This is consistent with previous reports that have demonstrated that addition of a variety of small epitope tags (c-Myc, H_7, or HA) either to the N- or C-terminus of caveolin-1 does not affect its correct targeting to caveolae membranes [11,35,44–46].

3.3. Differential effects of cell density, serum starvation, and growth factor stimulation on the expression of GFP-caveolin-1 and endogenous caveolin-1

In normal NIH 3T3 cells, we have recently shown that the expression of caveolin-1 is tightly controlled by cell density and exposure to serum factors [34]. Given that the GFP-caveolin-1 fusions are under the control of an exogenous promoter (CMV-based), we wondered whether the levels of the GFP-caveolins fusion proteins could be regulated by these stimuli. If this were the case, then this would reflect the existence of specific degradative mechanisms to control caveolin-1 levels. To test this hypothesis, we plated NIH 3T3 cells transiently transfected with the GFP-caveolin-1 fusions at different densities (sparse, sub-confluent, or confluent; see Section 2) we monitored the expression of GFP-caveolin-1 and endogenous caveolin-1 by Western blot analysis.

Fig. 3A shows that the expression of GFP-caveolin-1 is relatively independent of cell density as it is expressed to comparable levels in sparse, sub-confluent and confluent cells. In striking contrast, the levels of caveolin-1 are dramatically upregulated as the cells reach confluence. Thus, with regard to

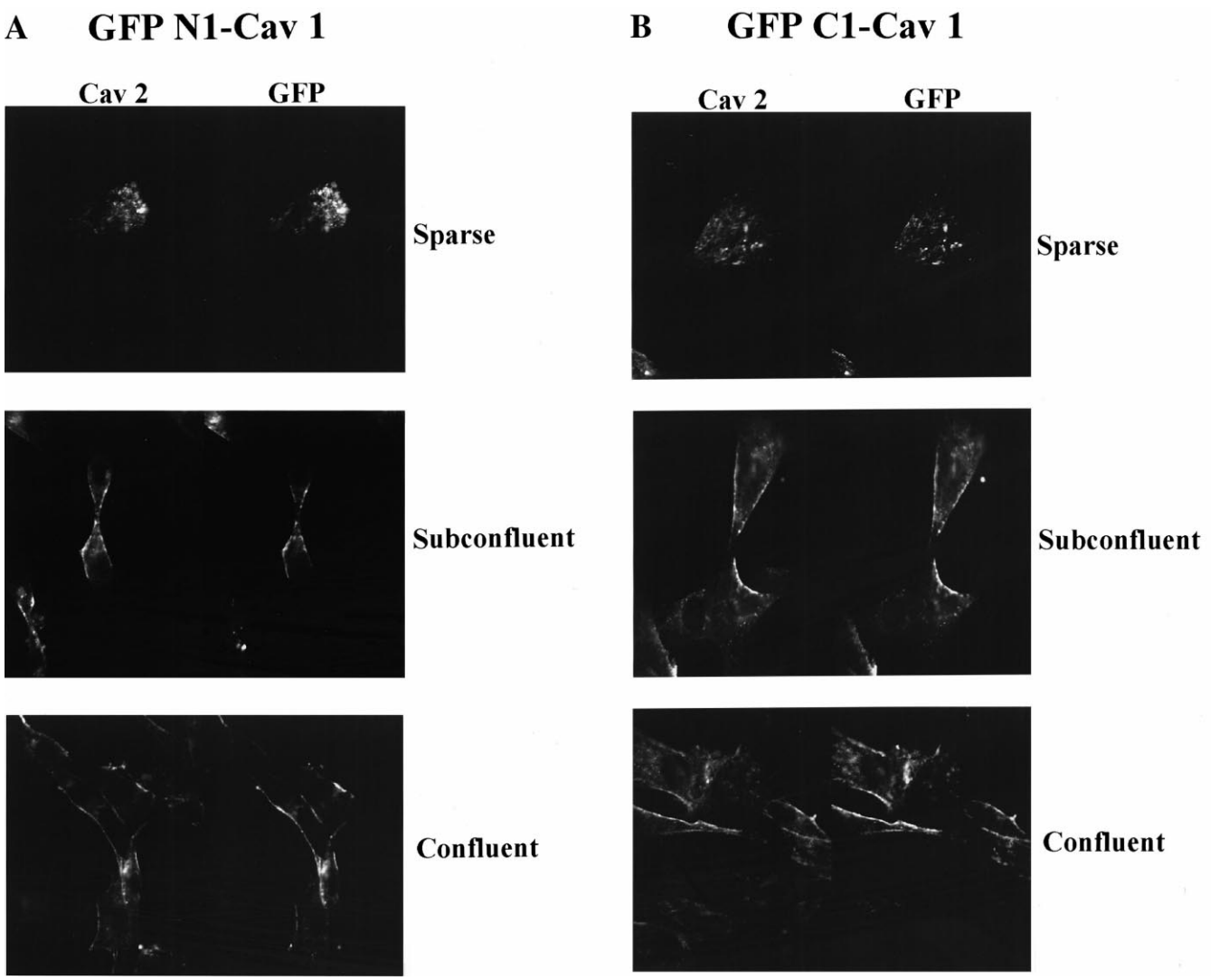

Fig. 6. Strict co-localization of GFP-caveolin-1 fusions with the endogenous caveolin-2 protein: effects of cell density. Dual-labeling with mono-specific antibodies directed against caveolin-2. Note that the distribution of caveolin-2 follows the distribution of the GFP-caveolin-1 fusion proteins. A: GFP N1-Cav-1; B: GFP C1-Cav-1. Left panels, caveolin-2 immunostaining; right panels, GPF-caveolin-1 fluorescence images.

the effects of cell density, the expression of GFP-caveolin-1 is unregulated while the expression of endogenous caveolin-1 remains tightly controlled. Fig. 3B shows the effects of serum deprivation on the expression levels of GFP-caveolin-1 fusion proteins and endogenous caveolin-1. Note that the expression of both GFP-caveolin-1 fusion proteins remains constant in the face of serum deprivation, while the levels of endogenous caveolin-1 are dramatically up-regulated.

Fig. 4 shows the effects of growth factor stimulation on the expression of caveolin-1. Expression of both GFP-caveolin-1 fusion proteins remains constant, while the levels of endogenous caveolin-1 are dramatically down-regulated in response to PDGF and FGF. Thus, the expression levels of exogenous GFP-caveolin-1 are clearly not affected by normal stimuli that regulate the expression of endogenous caveolin. This is consistent with the idea that these stimuli regulate caveolin-1 expression at the transcriptional level, rather than by stimulating or inhibiting a putative degradative pathway for caveolin-1, as we have postulated previously [23,31].

3.4. Localization of GFP-caveolin-1 fusions, and endogenous caveolin-1 in NIH 3T3 cells: effects of cell density

Both the expression level and the subcellular localization of endogenous caveolin-1 are controlled by cell density [34]. As cells reach confluence, the levels of endogenous caveolin-1 are up-regulated and shift from a random distribution over the entire cells surface to areas of cell-cell contact [34]. This is most dramatic in the case of sub-confluent cells that have established few cell-cell contacts. Are these density-dependent changes in the expression levels and the distribution of caveolin-1 controlled by similar or independent mechanisms?

To address this issue, we examined the subcellular distribution of GFP-caveolin-1 in transiently transfected NIH 3T3 cells plated at different cell densities (sparse, sub-confluent and confluent). Fig. 5 shows the localization of GFP-alone, GFP N1-caveolin-1, GFP C1-caveolin-1, and endogenous caveolin-1 in these cell populations. Note that the distribution of GFP alone is localized mainly to the cytosol and the nucleus and is independent of cell density. In contrast, the sub-

cellular distribution of both GFP-caveolin-1 fusions and endogenous caveolin-1 are strictly controlled by cell density. As the cells reach confluence, both GFP-caveolin-1 fusions and endogenous caveolin-1 are recruited to areas of cell-cell contact. This is most apparent in sub-confluent and confluent cells (compare phase images on the left with the corresponding fluorescence images on the right). These results clearly demonstrate that although the expression levels of GFP-caveolin-1 fusion proteins are not affected by cell density, their distribution is controlled by cell density and the formation of cell-cell contacts. Thus, the mechanisms that control the expression and localization of caveolin-1 in response to cell density are clearly separate and independent. These studies provide a novel living system with which to dissect the cell-density dependent mechanisms that control the localization of caveolin-1.

3.5. Localization of endogenous caveolin-1 in NIH 3T3 cells: co-localization with endogenous caveolin-2

NIH 3T3 cells co-express caveolins-1 and -2 where they are co-localized, form a stable hetero-oligomeric complex in vivo, and both are targeted to caveolae membranes [15]. Thus, we compared the subcellular distribution of GFP-caveolin-1 with the distribution of endogenous caveolin-2 at different cell densities.

Fig. 6 shows the distribution of GFP-caveolin-1 fusions and endogenous caveolin-2 in sparse, sub-confluent, and confluent NIH 3T3 cells. The localization of endogenous caveolin-2 was revealed by immunostaining with specific antibodies that recognize only caveolin-2, but not caveolin-1. These antibodies have been extensively characterized in a previous report [15]. Note that both GFP-caveolin-1 and endogenous caveolin-2 show strict co-localization at all three cell densities tested. As we have previously shown that endogenous caveolin-2 follows the distribution of endogenous caveolin-1 in response to changes in cell density [34], these results provide additional independent support for the idea that GFP-caveolin-1 is correctly localized in living cells and that it responds to the normal mechanisms that control the distribution of the caveolin-1 protein in living cells.

3.6. Caveolae, caveolins, and contact inhibition

Recently, we have employed an anti-sense approach to derive stable NIH 3T3 cell lines that express dramatically reduced levels of caveolin-1, but contain normal amounts of caveolin-2 [34]. As expected, caveolae were also down-regulated in these caveolin-1 anti-sense cell lines as seen by transmission electron microscopy [34]. Similarly, we and others have previously shown that expression of caveolin-1, but not caveolin-2, is sufficient to drive the formation of caveolae or caveolae-like vesicles in heterologous expression systems [15,17,19,20,35].

Interestingly, NIH 3T3 cells harboring anti-sense caveolin-1 exhibited a loss of contact inhibition, anchorage-independent growth in soft agar, tumor formation in immunodeficient mice, and appeared morphologically transformed, as seen by scanning electron microscopy [34]. Biochemically, these cells showed increased levels of activated MEK and ERK. These results suggest that down-regulation of caveolin-1 expression is sufficient to mediate a loss of contact inhibition, oncogenic transformation, and hyperactivation of the p42/44 MAP kinase cascade [34]. Importantly, this phenotype induced by targeted down-regulation of caveolin-1 expression was completely reversed when caveolin-1 protein levels were restored to normal by loss of the caveolin-1 anti-sense vector.

These observations may be related to the ability of caveolin-1 to positively regulate contact inhibition and growth arrest in normal cells. In support of this notion, we have shown that both the distribution and the expression of caveolin-1 are dramatically altered at confluence in normal NIH 3T3 cells [34]. These results are consistent with the idea that caveolin-1 may be important to mediate normal contact inhibition and to negatively regulate the activation state of the p42/44 MAP kinase cascade [34]. In addition, it has been shown that caveolins are most abundantly expressed in terminally differentiated cells such as endothelial cells, adipocytes, and muscle cells and are dramatically up-regulated during adipogenesis and myotube formation [14–16,47]. Thus, our current work with GFP-caveolin-1 fusion proteins provides a new living model system for elucidating the dynamic mechanisms underlying the density-dependent regulation of the distribution of caveolin-1 and how this relates to contact inhibition and the differentiated state.

Acknowledgements: This work was supported by an NIH Grant from the NCI (R01-CA-80250; to M.P.L.), and grants from the G. Harold and Leila Y. Mathers Charitable Foundation (to M.P.L.), the Charles E. Culpeper Foundation (to M.P.L.), and the Sidney Kimmel Foundation for Cancer Research (to M.P.L.).

References

[1] Lisanti, M.P., Scherer, P., Tang, Z.-L. and Sargiacomo, M. (1994) Trends Cell Biol. 4, 231–235.
[2] Okamoto, T., Schlegel, A., Scherer, P.E. and Lisanti, M.P. (1998) J. Biol. Chem. 273, 5419–5422.
[3] Couet, J., Li, S., Okamoto, T., Scherer, P.S. and Lisanti, M.P. (1997) Trends Cardiovasc. Med. 7, 103–110.
[4] Lisanti, M.P., Scherer, P.E., Vidugiriene, J., Tang, Z.-L., Hermanoski-Vosatka, A., Tu, Y.-H., Cook, R.F. and Sargiacomo, M. (1994) J. Cell Biol. 126, 111–126.
[5] Lisanti, M.P., Scherer, P.E., Tang, Z.-L., Kubler, E., Koleske, A.J. and Sargiacomo, M.S. (1995) Semin. Dev. Biol. 6, 47–58.
[6] Anderson, H.A., Chen, Y. and Norkin, L.C. (1996) Mol. Biol. Cell 7, 1825–1834.
[7] Montesano, R., Roth, J., Robert, A. and Orci, L. (1982) Nature 296, 651–653.
[8] Ikezu, T., Trapp, B.D., Song, K.S., Schegel, A., Lisanti, M.P. and Okamoto, T. (1998) J. Biol. Chem. 273, 10485–10495.
[9] Vey, M. et al. (1996) Proc. Natl. Acad. Sci. USA 93, 14945–14949.
[10] Smart, E.J., Ying, Y., Mineo, C. and Anderson, R.G.W. (1995) Proc. Natl. Acad. Sci. USA 92, 10104–10108.
[11] Song, K.S., Li, S., Okamoto, T., Quilliam, L., Sargiacomo, M. and Lisanti, M.P. (1996) J. Biol. Chem. 271, 9690–9697.
[12] Parton, R.G. (1996) Curr. Opin. Cell Biol. 8, 542–548.
[13] Scherer, P.E., Okamoto, T., Chun, M., Nishimoto, I., Lodish, H.F. and Lisanti, M.P. (1996) Proc. Natl. Acad. Sci. USA 93, 131–135.
[14] Tang, Z.-L. et al. (1996) J. Biol. Chem. 271, 2255–2261.
[15] Scherer, P.E. et al. (1997) J. Biol. Chem. 272, 29337–29346.
[16] Song, K.S. et al. (1996) J. Biol. Chem. 271, 15160–15165.
[17] Fra, A.M., Williamson, E., Simons, K. and Parton, R.G. (1995) Proc. Natl. Acad. Sci. USA 92, 8655–8659.
[18] Li, S., Song, K.S., Koh, S. and Lisanti, M.P. (1996) J. Biol. Chem. 271, 28647–28654.
[19] Li, S., Galbiati, F., Volonte, D., Sargiacomo, M., Engelman, J.A., Das, K., Scherer, P.E. and Lisanti, M.P. (1998) FEBS Lett. 434, 127–134.
[20] Engelman, J.A., Wycoff, C.C., Yasuhara, S., Song, K.S., Okamoto, T. and Lisanti, M.P. (1997) J. Biol. Chem. 272, 16374–16381.

[21] Sargiacomo, M., Scherer, P.E., Tang, Z.-L., Kubler, E., Song, K.S., Sanders, M.C. and Lisanti, M.P. (1995) Proc. Natl. Acad. Sci. USA 92, 9407–9411.
[22] Li, S., Couet, J. and Lisanti, M.P. (1996) J. Biol. Chem. 271, 29182–29190.
[23] Engelman, J.A. et al. (1998) J. Biol. Chem. 273, 20448–20455.
[24] Engelman, J.A., Chu, C., Lin, A., Jo, H., Ikezu, T., Okamoto, T., Kohtz, D.S. and Lisanti, M.P. (1998) FEBS Lett. 428, 205–211.
[25] Li, S., Okamoto, T., Chun, M., Sargiacomo, M., Casanova, J.E., Hansen, S.H., Nishimoto, I. and Lisanti, M.P. (1995) J. Biol. Chem. 270, 15693–15701.
[26] Couet, J., Li, S., Okamoto, T., Ikezu, T. and Lisanti, M.P. (1997) J. Biol. Chem. 272, 6525–6533.
[27] Couet, J., Sargiacomo, M. and Lisanti, M.P. (1997) J. Biol. Chem. 272, 30429–30438.
[28] Oka, N., Yamamoto, M., Schwencke, C., Kawabe, J., Ebina, T., Couet, J., Lisanti, M.P. and Ishikawa, Y. (1997) J. Biol. Chem. 272, 33416–33421.
[29] Minetti, C. et al. (1998) Nature Genet. 18, 365–368.
[30] Garcia-Cardena, G., Martasek, P., Siler-Masters, B.S., Skidd, P.M., Couet, J.C., Li, S., Lisanti, M.P. and Sessa, W.C. (1997) J. Biol. Chem. 272, 25437–25440.
[31] Koleske, A.J., Baltimore, D. and Lisanti, M.P. (1995) Proc. Natl. Acad. Sci. USA 92, 1381–1385.
[32] Engelman, J.A., Zhang, X.L. and Lisanti, M.P. (1998) FEBS Lett. 436, 403–410.
[33] Engelman, J.A., Zhang, X.L., Galbiati, F. and Lisanti, M.P. (1998) FEBS Lett. 429, 330–336.
[34] Galbiati, F., Volonte, D., Engelman, J.A., Watanabe, G., Burk, R., Pestell, R. and Lisanti, M.P. (1998) EMBO J. 17, 6633–6648.
[35] Scherer, P.E., Tang, Z.-L., Chun, M.C., Sargiacomo, M., Lodish, H.F. and Lisanti, M.P. (1995) J. Biol. Chem. 270, 16395–16401.
[36] Sargiacomo, M., Sudol, M., Tang, Z.-L. and Lisanti, M.P. (1993) J. Cell Biol. 122, 789–807.
[37] Sargiacomo, M., Scherer, P.E., Tang, Z.-L., Casanova, J.E. and Lisanti, M.P. (1994) Oncogene 9, 2589–2595.
[38] Scherer, P.E., Lisanti, M.P., Baldini, G., Sargiacomo, M., Corley-Mastick, C. and Lodish, H.F. (1994) J. Cell Biol. 127, 1233–1243.
[39] Lisanti, M.P., Tang, Z.-T., Scherer, P. and Sargiacomo, M. (1995) Methods Enzymol. 250, 655–668.
[40] Schnitzer, J.E., Oh, P., Jacobson, B.S. and Dvorak, A.M. (1995) Proc. Natl. Acad. Sci. USA 92, 1759–1763.
[41] Corley-Mastick, C., Brady, M.J. and Saltiel, A.R. (1995) J. Cell Biol. 129, 1523–1531.
[42] Robbins, S.M., Quintrell, N.A. and Bishop, M.J. (1995) Mol. Cell. Biol. 15, 3507–3515.
[43] Smart, E., Ying, Y.-S., Conrad, P. and Anderson, R.G.W. (1994) J. Cell Biol. 127, 1185–1197.
[44] Kurzchalia, T., Dupree, P., Parton, R.G., Kellner, R., Virta, H., Lehnert, M. and Simons, K. (1992) J. Cell Biol. 118, 1003–1014.
[45] Dietzen, D.J., Hastings, W.R. and Lublin, D.M. (1995) J. Biol. Chem. 270, 6838–6842.
[46] Li, S., Song, K.S. and Lisanti, M.P. (1996) J. Biol. Chem. 271, 568–573.
[47] Way, M. and Parton, R. (1995) FEBS Lett. 376, 108–112.